Journal of Hazardous Materials 405 (2021) 124206

Contents lists available at ScienceDirect

Journal of Hazardous Materials

journal homepage: www.elsevier.com/locate/jhazmat

Research Paper

# Addition of nanoparticles increases the abundance of mobile genetic elements and changes microbial community in the sludge anaerobic digestion system

Yanru Zhang [a,b], Rui Xu [c,d], Yinping Xiang [a,b], Yue Lu [a,b], Meiying Jia [a,b], Jing Huang [e], Zhengyong Xu [f], Jiao Cao [a,b], Weiping Xiong [a,b,*], Zhaohui Yang [a,b,*]

[a] College of Environmental Science and Engineering, Hunan University, Changsha 410082, PR China
[b] Key Laboratory of Environmental Biology and Pollution Control (Hunan University), Ministry of Education, Changsha 410082, PR China
[c] Guangdong Key Laboratory of Integrated Agro-environmental Pollution Control and Management, Guangdong Institute of Eco-environmental Science Technology, Guangzhou 510650, PR China
[d] National-Regional Joint Engineering Research Center for Soil Pollution Control and Remediation in South China, Guangzhou 510650, PR China
[e] Hunan Academy of Forestry and State Key Laboratory of Utilization of Woody Oil Resource, Changsha 410004, PR China
[f] Hunan Provincial Science and Technology Affairs Center, Changsha 410013, PR China

ARTICLE INFO

*Keywords:*
Mobile genetic elements
Nanoparticles
Mesophilic anaerobic digestion
Potential host

ABSTRACT

This study explored the fate of mobile genetic elements (MGEs) in anaerobic digestion (AD) system with four nanoparticles (NPs) added, including carbon NPs, $Al_2O_3$ NPs, ZnO NPs, and CuO NPs. 16S rRNA amplicon sequencing and quantitative PCR to investigate the microbial community, MGEs abundance and the potential host in the AD process. The results of high-throughput sequencing showed that ZnO NPs and CuO NPs significantly reduced the microbial diversity and significantly changed the microbial community structure. Simultaneously, the absolute abundance of MGEs increased by 145.01%, 159.67%, 354.70%, and 132.80% on the carbon NPs, $Al_2O_3$ NPs, ZnO NPs, and CuO NPs. The enrichment rate *of tnpA*-03 in ZnO NPs group was the highest, which could reach up to 2854.80%. Co-occurrence analysis revealed that Proteobacteria harbored the vast majority of MGEs followed by Firmicutes. Redundancy analysis and variation partitioning analysis showed that metabolites were the main factors that shifted the succession of bacterial communities. Moreover, there were significant positive correlations between metabolites and part MGEs (such as *tnpA*-01, *tnpA*-02, *tnpA*-03, *tnpA*-04, *tnpA*-05, *tnpA*-07 and *IS*CR1). This study provides a new perspective that NPs increase the risk of antibiotic resistance through MGEs during AD process.

## 1. Introduction

Antibiotics are widely used to maintain the health of humans and animals, because of their ability to treat infectious diseases (W.H. Organization, 2015; Yan et al., 2020). However, the overuse and misuse of antibiotics have also resulted in the spread of antibiotic-resistant bacteria (ARB) and antibiotic resistance genes (ARGs) in the environment (Xu et al., 2020c). Mobile genetic elements (MGEs) are the elements that promote DNA mobility within or between cells, including plasmids, transposons, insertion sequences and integrons (Nolivos et al., 2019). Insertion sequences and transposons are discrete DNA fragments, which that could move the associated resistance genes to new positions in the same or different DNA molecules within a cell. Integrons can be used to transfer resistance genes between identified sites via site-specific recombination. These MGEs together facilitate horizontal gene transfer (HGT), thereby promoting the acquisition and dissemination of ARGs. The capture, accumulation and transmission of resistance genes are mainly due to the action of MGEs. After the selective pressure has been removed, the intact DNA may survive and transfer ARGs to other bacteria via HGT through MGEs, so ARGs can widely exist in environment, regardless in living or dead cells (Partridge et al., 2018a). Since these MGEs usually have multiple copies at different locations in the genome, they could promote sequence exchange between identical or related fragments (Partridge et al., 2018b). The interaction among the different MGE is the driving force for the rapid evolution of multi-resistant pathogens. Thus, MGEs detection could be used to assess the

* Corresponding authors at: College of Environmental Science and Engineering, Hunan University, Changsha 410082, PR China
*E-mail addresses:* xiongweiping@hnu.edu.cn (W. Xiong), yzh@hnu.edu.cn (Z. Yang).

https://doi.org/10.1016/j.jhazmat.2020.124206
Received 11 August 2020; Received in revised form 30 September 2020; Accepted 5 October 2020
Available online 8 October 2020

potential transmission risk of antibiotic resistance (Hall and Stokes, 1993).

Most of the urban wastewater treatment plants (WWTPs) receive domestic wastewater from urban residents, which contains high concentrations of antibiotics. Therefore, WWTPs are considered as potential sources of resistance genes and MGEs in the environment (Rizzo et al., 2013). There was no special process designed for removing resistance genes and MGEs in traditional WWTPs and the abundance of resistance genes and MGEs in waste activated sludge even increased after the biological wastewater treatment process (Di Cesare et al., 2016; Liu et al., 2020). From the perspectives of energy conservation and resource recovery in WWTPs, anaerobic digestion (AD) is considered as a successful technologies for sustainable alternative energy recovery (Xu et al., 2019). During AD process, the organic material of waste activated sludge will be converted into the biogas by bacteria. AD was considered to hinder the transmission of antibiotic resistance in waste activated sludge (Yan et al., 2019). However, an increasing number of studies have documented that AD process can only reduce part of resistance genes (Zhang et al., 2020). One potential reason for this behavior is that the remaining survivors related to resistance genes experienced a significant resurgence due to the micro-environment generated from AD, which can lead to HGT of antibiotic resistance through MGEs (Wallace et al., 2018). However, in existing researches, there have been lack of the studies on the fates of MGEs in AD systems. A knowledge gap remains regarding how MGEs in waste activated sludge respond to different AD processes.

Engineered nanoparticles (NPs) are widely used in various fields. Carbon NPs have been used in advanced treatment of sewage sludge. This is because carbon NPs will gradually be converted into bio-activated carbon in the long-term use process, which enables the pollutant to be degraded by microorganisms (Sun et al., 2020). Engineered metal oxide NPs, such as $Al_2O_3$ NPs, ZnO NPs and CuO NPs, have been mass-produced and applied to industry and individuals due to their catalytic activities, photoelectric performance, and antibacterial properties (Yuan et al., 2020). $Al_2O_3$ NPs are widely used in water absorbent materials, antibacterial materials and abrasive materials. ZnO NPs have been widely used in biomedical field, such as drug delivery and biological imaging probes. CuO NPs are widely produced as a by-product of chemical mechanical polishing in semiconductor industry. As a result, these four NPs are inevitably released into the industrial and municipal wastewater. The concentrations of engineered NPs in WWTPs could reach to mg/L (Kapoor et al., 2018; Sun et al., 2016). The cytotoxicity to the biological activities from engineered NPs has become a new emerging environmental issue (Yuan et al., 2019). The presence of NPs is considered as a stimulus to sludge microbes, which may have adverse effects on the AD performance by inhibiting hydrolysis and methanation steps (Mu and Chen, 2011). NPs could cause ARB death, while the cell permeability of ARB is increased when exposed to highly abundant NPs, thereby enhancing the antibiotic resistance of ARB. Bacteria can sense stimuli and make transcriptional responses through signal transduction pathway (Wösten et al., 2000). Thus, the presence of NPs may also trigger the transduction pathways in sludge microbes. It is plausible to speculate that stimulated transduction pathways might affect the associated behaviors of MGEs and change the distribution of MGEs. Several studies have indicated that NPs can promote HGT of plasmid borne ARGs (Qiu et al., 2012). In addition, it has been proved that some bacteria were the carriers of MGEs. NPs can cause succession of bacterial community carrying MGEs, which is responsible factor for the variation of MGEs abundance.

In conclusion, most studies paid attention to the effect of engineered NPs on the AD performance (Xiang et al., 2019; Wang et al., 2019; Li et al., 2020). These studies rarely highlight how various NPs affected microbial community, MGEs propagation and bacteria carrying-MGE in AD system. Especially, previous studies on the changes of MGEs during AD system mainly focused on integrons, while studies on other MGEs were less. It is necessary to further study the NPs in waste activated sludge and understand the potential hazards of NPs-enhanced MGEs propagation in AD system. The microbial community, MGEs abundance, potential host of MGEs, and various environmental parameters need to be investigated as fundamental factors when studying MGEs propagation in AD systems with different NPs added. This study investigated the effect of four engineered NPs (including carbon NPs, $Al_2O_3$ NPs, ZnO NPs, and CuO NPs) on MGEs in the mesophilic AD system. The purposes of this study were to (1) reveal the effects of microbial community and MGEs among AD reactors with or without NPs added by 16S rRNA amplicon sequencing and quantitative PCR, (2) identify the potential host of MGEs and (3) find out the performance parameters that affect the abundance of MGEs and the structure of bacterial community. This study extends current understanding that the release of NPs may influence the propagation of ARGs in AD system.

## 2. Materials and methods

### 2.1. Preparation of inoculum sludge, feed sludge and conductive nanoparticles

Feed and inoculum sludge were both collected from a local WWTP in Changsha, China. Inoculum sludge was the anaerobic acclimated sludge under the mesophilic environment, and many anaerobic microorganisms are enriched in inoculum sludge. Feed sludge provided necessary organic matter for anaerobic microorganisms to carry out metabolic activities. pH of feed and inoculum sludge ranged from 6.31 to 7.58. Total solid contents were 30.33 g/L (inoculum) and 90.67 g/L (feed sludge). Details of inoculum and feed sludge could be found in Table 1. Four types of engineered NPs were used in this study, including carbon NPs (99.5%, 30 nm), $Al_2O_3$ NPs (99.9% metals basis, 30 nm), ZnO NPs (99.9% metals basis, 30 nm) and CuO NPs (99.5%, 40 nm). All these engineered NPs were purchased from Shanghai Macklin Biochemical Co., Ltd., China.

### 2.2. Setup of anaerobic digesters

Five groups marked as A (blank), B (carbon NPs), C ($Al_2O_3$ NPs), D (ZnO NPs) and E (CuO NPs). The dosage of NPs was 50.0 mg $g^{-1}$ TS in different digesters. Lab scale AD was adopted in this study. The working volume of the digesters is 3 L, including 2 L of inoculum sludge and 1 L of digestive materials initially. There is a silica gel plug at the top of each reactor, and two holes are drilled on the silica gel plug to connect a gas collecting bag and a sludge sample tube, respectively. Before the experiment was started, nitrogen was pumped into the reactors for 20 min to create an anaerobic environment. All reactors were operated in a constant temperature water bath at 35 °C. When the daily biogas production is less than 5% of the previous day's biogas production, the experiment is over. Operational temperature of reactors was manipulated by an electronical water-bath. Three parallel digesters were set for each group.

### 2.3. Sample collection and physico-chemical analysis

Five groups of digestion samples were collected after the experiment.

**Table 1**
Main characteristics of feed sludge and inoculum sludge used in this study.

| Parameter | Feed | Inoculum |
|---|---|---|
| pH | 6.31 ± 0.01 | 7.58 ± 0.02 |
| Moisture (%) | 91.45 ± 0.04 | 96.90 ± 0.12 |
| TS (g $L^{-1}$ substrate) | 90.67 ± 6.55 | 30.33 ± 1.89 |
| VS (g $L^{-1}$ substrate) | 35.00 ± 2.45 | 10.00 ± 0.81 |
| sCOD (g $L^{-1}$) | 3.62 ± 0.30 | 0.60 ± 0.03 |
| Total polysaccharides (g $L^{-1}$) | 0.378 ± 0.011 | 0.047 ± 0.014 |
| Protein (g $L^{-1}$) | 0.12 ± 0.03 | 0.11 ± 0.01 |
| $NH_4^+$-N (g $L^{-1}$) | 84.06 ± 0.53 | 36.99 ± 1.36 |

Each sample was divided into two parts. One part was used to determine the physico-chemical parameters. The other part was freeze-dried before molecular analysis and stored in the sterile centrifuge tubes at − 80 °C. The main AD parameters, including pH, biogas yield, total solids (TS), volatile solids (VS), moisture, soluble chemical oxygen demand (SCOD), total polysaccharides, protein and volatile fatty acids (VFAs), were measured in triplicates to monitor the AD performance. Detailed measurement methods were listed in our previous work (Xu et al., 2018a; Zhang et al., 2019b). In short, daily biogas yield was measured by the drainage method. Digested samples were centrifuged (5000 rpm, 15 min) and filtered (0.45 μm) to measure pH, sCOD, total polysaccharides and protein. VFAs were detected by the gas chromatograph (GC, Shimazu 2010) with a flame ionization detector (Liu et al., 2019a). All measurements were in triplicate.

### 2.4. DNA extraction and quantitative PCR (qPCR) of MGEs

The genomic DNA of each freeze-dried sludge sample (0.5 g) was extracted by the E.Z.N.A.® Soil DNA Kit (Omega Bio-tek, Norcross, GA, USA) which was in line with the manufacture introduction. Genomic DNA was qualified and quantified by gels electrophoresis and Qubit. Detailed measurement methods were shown in the previous work (Xu et al., 2017). Quantitative PCR (qPCR) is a feasible method to detect gene fragment concentrations in complex environmental samples. Therefore, qPCR was used to quantify the screened MGEs in this study. Based on the existing study (Zhu et al., 2017), eleven MGEs with higher detection frequency in activated sludge were selected for quantitative analysis. These MGEs including one integron (*intI*1), nine transferases (*IS613*, *tnpA*-01, *tnpA*-02, *tnpA*-03, *tnpA*-04, *tnpA*-05 and *tnpA*-07, *Tp*614 and *Tn*916/1545), one insertion sequences (*IS*CR1) and microbial 16S rRNA genes for bacteria were selected. The forward and reverse primer sequences expected amplicon size and primer annealing temperature of gene targets selected in this study were listed in Table S1 of supplementary material. The standard curve and amplification efficiency of t11 selected MGEs and bacteria by qPCR were listed in Table S2.

The qPCR of 11 selected MGEs and bacteria was performed on iQ5 real-time PCR thermocycler (BIO-RAD, USA) with Super Real fluorescence premixing (SYBR Green) kit. Each target gene was quantified in triplicate for each sample by the purified DNA template calibration curve, which had been amplified by conventional PCR and negative control. The reaction mixture (20 μL) was formed with 10 μL of 2 × Power PreMix (Tiangen, China), 0.6 μL of forward/reverse primer (10 μM), 1.0 μL of template DNA, and 7.8 μL of RNase-Free dd$H_2O$. The temperature of melting curves analysis was between 50 °C and 95 °C with 0.5 °C/30 s per cycle. Bacterial 16S rRNA genes was selected as the internal reference gene to minimize the basis caused by different bacterial abundance (Xu et al., 2018b).

### 2.5. 16S rRNA amplicon sequencing

The bacterial community was analyzed by the primers 338F (5′-ACTCCTACGGGAGGCAGCA-3′)/806R (5′- GGACTACHVGGGTWTCTAAT-3′) targeting the V3-V4 hyper variable regions. And the primers 524F (5′- TGYCAGCCGCCGCGGTAA-3′)/958R (5′- YCCGGCGTTGAVTCCAATT) targeting the V4-V5 hyper variable regions were selected for archaeal community analysis as described in the previous study (Xu et al., 2018a). Raw sequences were deposited to NCBI and the project is No. SRP212983.

### 2.6. Statistical analysis

UCHIME was used to identify and remove the chimeric 16S rRNA amplicon sequences. The clean 16S rRNA amplicon sequences were clustered into operational taxonomic units (OTUs) at 97% sequence identity by UCLUST. Microbial diversity and relative abundance were analyzed in the Microbiome Analyst platform (http://www.microbiomeanalyst.ca/) (Dhariwal et al., 2017). The differential analysis between two groups was conducted in STAMP. The relationships among performance parameters, bacterial genera and MGEs were explored by Spearmans' rank correlation coefficient. The bacterial genes with relative abundances > 1% and MGEs were subjected to Spearman's correlation analysis. The correlation between bacterial genes and MGEs was greater than 0.8 ($P < 0.005$), which was considered as a significant pairwise correlation between two nodes (Xu et al., 2020a). The co-occurrence network of MGE-bacteria was visualized using the Gephi (V0.9.1) toolkit. Redundancy analysis (RDA) was performed using Canoco 5.0. The "vegan" packages in R software (version 3.3.0) were applied to explore the variation partitioning analysis (VPA). HemI 1.0 was used to conducted heat-map.

## 3. Results and discussion

### 3.1. General digestion characterization

The digesters of five groups were operated at mesophilic condition for 36 days. The general digestion performances were summarized in Table 2. The four NPs did not change the pH of these digesters dramatically (ranged from 7.09 ± 0.11 to 7.37 ± 0.31) at the end of the experiment. The average accumulative biogas yield in five groups were 201.93 ± 12.30 (blank), 313.56 ± 11.29 (carbon NPs), 296.97 ± 20.16 ($Al_2O_3$ NPs), 24.79 ± 3.36 (ZnO NPs) and 194.26 ± 9.79 (CuO NPs) mL $g^{-1}$ $VS_{added}$, respectively. Compared with the group A, the cumulative biogas yield increased by 47.07% and 55.28% in group B and group C, while decreased by 90.2% and 3.80% in group D and group E, respectively. By the end of the digestion, the accumulate biogas yield of five groups could be also consist with the solid content (moisture, TS and VS) and the metabolites concentrations (SCOD, VFAs, protein and soluble polysaccharide). The solid content and metabolites concentrations of group B and group C were lower than that of group A, while those parameters of group D and group E were higher than that of group A.

Several studies have reported that there is a range of concentration for carbon-based NPs that can be feasible for enhancing AD performance (Li et al., 2020; Xu et al., 2020b). A study has shown that addition of 200 mg $L^{-1}$ nano-magnetic carbon could significantly reduce the accumulation of VFAs, thereby avoiding acidification in AD process. The methane productions were enhanced by 33.4% in the nano-magnetic carbon systems, compared with the blank digester (Li et al., 2020). Carbon NPs has been demonstrated to enriched hydrogen-utilizing methanogens and Geobactor which could enhance the electron exchange efficiency between syntrophs and methanogens by direct interspecies electron transfer. In addition, carbon NPs also promoted the conversion of $CO_2$ to methane, shorten the lag time of initiating methane yield, and increased methane yield (Yang et al., 2017). There were limited researches on the influence of $Al_2O_3$ NPs on anaerobic digestibility, and almost all the conclusions were that $Al_2O_3$ NPs has no inhibition on AD biogas production (Gonzalez-Estrella et al., 2013; Vodovnik et al., 2012; Mu et al., 2011). This may be due to the weak solubility of $Al_2O_3$ NPs. In addition, the increase in biogas production caused by $Al_2O_3$ NPs may be due to its hexagonal crystal structure. This structure has large specific surface area and appropriate pore structure. Therefore, $Al_2O_3$ NPs can provide a carrier of anaerobic medium for microorganisms. Studies have shown that when the concentration of ZnO NPs in the AD reactor reached 30 mg $g^{-1}$ TSS, the methane production was 77.2% of the control group (Mu et al., 2011). The CuO NPs with a concentration of 250 mg $L^{-1}$ could decrease the normalized methanogenic activity to 79.9% of the control group (Gonzalez-Estrella et al., 2013). Previous studies have shown that the corrosion and dissolution of the NPs release toxic $Cu^{2+}$ and $Zn^{2+}$, which is the main mechanism of methanogenic inhibition by CuO NPs and ZnO NPs (Mu et al., 2011). $Zn^{2+}$ can inhibit the protein hydrolysis, resulting in the decrease of VFAs production rate (Zhang et al., 2017). $Cu^{2+}$ also inhibited the acetolactic methanogens (Gonzalez-Estrella et al., 2013). A

**Table 2**
Summary of digestion parameters for each group.

| Parameter | A | B | C | D | E |
|---|---|---|---|---|---|
| pH | 7.35 ± 0.12 | 7.37 ± 0.31 | 7.36 ± 0.22 | 7.09 ± 0.11 | 7.22 ± 0.18 |
| Cumulative biogas yield (mL $g^{-1}VS_{added}$) | 201.93 ± 12.30 | 313.56 ± 11.29 | 296.97 ± 20.16 | 24.79 ± 10.36 | 194.26 ± 9.79 |
| Moisture (%) | 93.82 ± 0.33 | 94.19 ± 2.09 | 95.01 ± 0.16 | 91.01 ± 3.25 | 89.79 ± 5.63 |
| TS (g $L^{-1}$ substrate) | 62.50 ± 4.80 | 58.00 ± 2.05 | 49.5 ± 2.65 | 109.25 ± 6.26 | 95.00 ± 3.67 |
| VS (g $L^{-1}$ substrate) | 17.75 ± 2.22 | 17.5 ± 1.91 | 17.00 ± 1.15 | 18.75 ± 0.50 | 20.00 ± 0.82 |
| SCOD (mg $L^{-1}$) | 642.56 ± 54.78 | 515.74 ± 12.41 | 560.83 ± 32.80 | 3386.57 ± 23.95 | 1503.05 ± 11.03 |
| Total polysaccharides (mg $L^{-1}$) | 42.80 ± 3.34 | 26.96 ± 1.58 | 31.22 ± 2.98 | 150.93 ± 1.52 | 45.85 ± 3.13 |
| Protein (mg $L^{-1}$) | 86.14 ± 2.09 | 47.5 ± 1.88 | 77.05 ± 2.85 | 512.27 ± 22.38 | 511.14 ± 28.49 |
| VFAs (mg $L^{-1}$) | 16.02 ± 2.61 | 11.5945 ± 1.21 | 11.767 ± 1.05 | 1488.10 ± 23.67 | 322.18 ± 5.74 |

higher dose of ZnO NPs and CuO NPs can inhibit the hydrolysis-acidification of AD.

SCOD, VFAs, protein and total polysaccharide are metabolites in methane-producing processes, which could represent the degree of sludge digestion (Zhang et al., 2019b). Carbon NPs and $Al_2O_3$ NPs could enhance the activity of anaerobic microorganisms through direct interspecific electron transfer or provide anaerobic environment, thus accelerate the organic matter degradation. As carbon NPs and $Al_2O_3$ NPs could promote biogas production, the substrate digestion was more thorough, so the concentration of metabolites is lower than the control group. On the contrary, ZnO NPs and CuO NPs could inhibit the degradation rate of soluble protein and soluble polysaccharide, which may be due to the inhibition of protease and cellulose activity by the ZnO NPs and CuO NPs (Gonzalez-Estrella et al., 2013). Protease and cellulase are the key enzymes in the hydrolysis stage, which could enhance the hydrolysis of soluble protein and soluble polysaccharide (Mu and Chen, 2011). Therefore, the increase of SCOD, VFAs, protein and total polysaccharide accumulation verified the inhibition of the biogas production ability in AD process with the addition of ZnO NPs and CuO NPs.

### 3.2. Effects of four NPs exposure on the abundance of MGEs

Different NPs have varying degrees of influence on the MGEs abundance. The absolute abundance of MGEs significantly increased in the digesters with NPs added (Fig. 1a). The total absolute abundance of MGEs was $8.41 \times 10^5$ copies $\mu L^{-1}$ in group A, in which *IS613* was dominant, and the absolute abundance of *IS*613 was $3.90 \times 10^5$ copies $\mu L^{-1}$. The absolute abundance of MGEs increased by 145.01%, 159.67%, 354.70%, and 132.80% in the group B, C, D and E, respectively, compared to group A. The total absolute abundance of MGEs was highest in group C. *IS*613 was also dominant in group B, C and D, but the abundance of *IS*613 was significantly decreased in the group E. It is worth noting that in group D, *tnpA*-02 and *tnpA*-04 also dominated. The variation trend of MGEs relative abundance was consistent with that of absolute abundance. The relative abundance of almost all MGEs were enriched in the groups with NPs added, while the relative abundance of *IS*613 decreased in the group E (Fig. 1b).

The enrichment efficiency of all MGEs was calculated, yielding 58.09–129.29% of *IS*613, 114.90–502.50% of *tnpA*-04, 215.64–562.30% of *tnpA*-02, 90.41–758.04% of *tnpA*-05, 270.05–620.23% of *intI*1, 91.76–336.61% of *tnpA*-07, 98.89–403.83% of *tnpA*-01, 500.03–1412.22% of *Tn*916/1545, 148.81–2854.80% of *tnpA*-03, 46.71–67.06% of *Tp*614, and 11.06–662.01% of *ISCR*1 (Fig. 1c). *tnpA*-03 had the highest enrichment rate in group D. The abundance of MGEs in ZnO NPs group was significantly increased, suggesting that MGEs enrichment would occur if ZnO NPs were added during anaerobic digestion. The addition of 50 mg $g^{-1}$ TS NPs (carbon NPs, $Al_2O_3$ NPs, ZnO NPs and CuO NPs) significantly increased the MGEs abundance in the anaerobic digestion product.

A large number of studies have shown that MGEs contributed to the migration of antibiotic resistance in different environmental intervals. Transposases were reported to be encoded with tetracycline resistance genes and macrolide resistance genes (Okitsu et al., 2005). As a marker of anthropogenic pollution (Hall and Stokes, 1993), *intI*1 is often detected in AD systems. *tnpA*-02 and *tnpA*-05 were strongly associated with the resistance genes in different substrates. Studies have shown that nano-carbon can promote the appearance of multibacterial zoogloea, resulting in the cell membrane contact of different bacterium (Qiu et al., 2012). $Al_2O_3$ NPs could promote conjugative transfer of ARGs from *Escherichia coli* to *Streptomyces* (Liu et al., 2019b). Both carbon NPs and $Al_2O_3$ NPs provided a suitable environment for the conjugative transfer of resistance gene from donor bacteria to recipients or other bacteria via plasmid-mediated conjugation in environment (Sun et al., 2020). The conjugative frequency of antibiotic resistance plasmid RP4 showed a marked increase in bacterial, which exposure to ZnO NPs at sublethal concentrations (1–10 mg $L^{-1}$) (Wang et al., 2018). CuO NPs and ZnO NPs could increase both the abundance and the diversities of plasmids. Moreover, compared with the control group, the integrons abundance increased by 92% in CuO NPs group and 58.67% in ZnO NPs group (Huang et al., 2019). The gene cassettes, which reside in *intI*1, would integrate and expresses more than a hundred subtypes of ARGs (Gillings

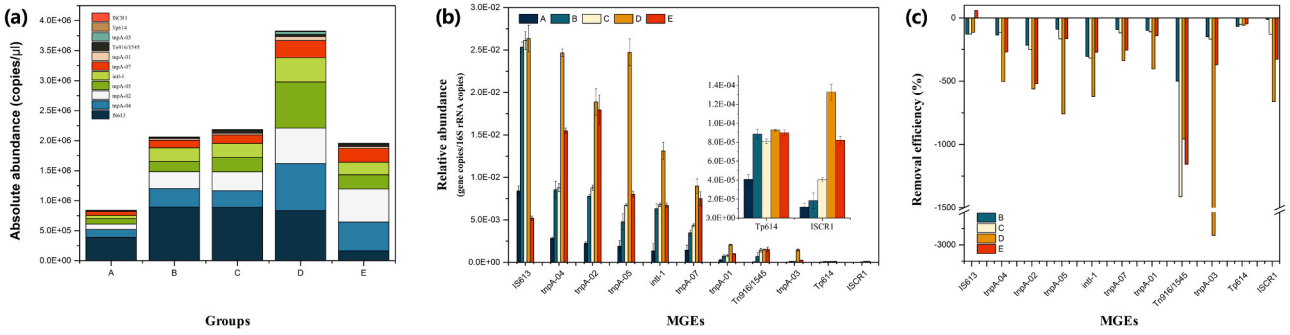


**Fig. 1.** The absolute abundance (a) and relative abundance (b) of MGEs in five groups. The removal efficiency of MGEs in carbon NPs group, $Al_2O_3$ NPs group, ZnO NPs group, and CuO NPs group (c). The relative abundance of MGEs detected in this study was normalized by the 16S rRNA gene copies to minimize the basis caused by different microbial abundance.

et al., 2008). Insertion sequences linked with respect to non-cassette ARGs played a significant role in their migration. For instance, non-cassette ARGs such as *dfr*A and *qnr* could form complex class 1 integrons mediated by the *IS*CR1 family (Toleman et al., 2006). Consequently, this study suggested that more ARGs might be migrated among bacteria with the increased abundance of MGEs in AD system with the NPs added.

NPs enhanced horizontal transfer of resistance gene by regulating gene expression through the nanoparticle-specific effect. The reason for this phenomenon was the increase of bacterial cell permeability after bacteria exposed to NPs (Wang et al., 2018). The presence of NPs initiated bacterial cell signaling such as quorum sensing, pili synthesis and metal tolerance, which in turn leads to the succession of bacteria community (ARGs hosts), enhanced transgenosis potential and stimulated co-selection. For example, functional pili were suggested to play major roles in the transport of MGEs, which could even initiate conjugal DNA transfer (Harshey, 2003). NPs stimulated the synthesis of regulatory signaling responsible for chemosensory pili and type IV fimbriae. KOs proteins such as ChpA and Pil were all increased with NPs, indicating that biogenesis and transcription of type IV pili was promoted (Kaiser, 2000). Besides, NPs also promoted the synthesis of flagella, which facilitate the movability of bacteria. Therefore, in the presence of NPs, the connection of ARG hosts to the potential receptors became easier. In addition, the intracellular reactive oxygen species content increased after adding ZnO NPs and CuO NPs. Reactive oxygen species facilitated the mRNA expression levels of conjugative genes by suppressing global regulation genes. Simultaneously, it also stimulated the expression of *int*A, a conjugation related gene, which eventually increased the abundance of MGEs (Liu et al., 2019b). This could explain why ZnO NPs and CuO NPs have a more significant enrichment effect on MGEs during AD process.

### 3.3. Effects of four NPs exposure on the variation of microbial community

According to 16S rRNA gene Miseq-PE250 sequencing data, the variation of microbial communities in the five groups was explored. The microbial community composition at phylum and genus level were displayed in Fig. 2a-d. Among the five identified archaeal phyla, the phylum Euryarchaeota was the dominant member with a relative abundance of 97.76–98.63%. Members of the phyla Firmicutes (accounting for 28.59–29.51% of total reads), Proteobacteria (15.55–16.67%), and Bacteroidetes (6.37–7.82%) were the dominant bacterial phylum in all groups. There were 4 archaea phyla and 9 bacterial phyla statistically significant differences among five groups (Fig. 1e and f). The relative abundance of Euryarchaeota ($P = 0.027$), Crenarchaeota ($P = 0.023$), Asgardaeota ($P = 0.036$), Thaumarchaeota ($P = 0.028$) were all significantly difference in the five groups. Among the top 10 bacterial phyla in relative abundance, there were significant differences in the nine phyla (Firmicutes, Proteobacteria, Bacteroidetes, Patescibacteria, Actinobacteria, Acidobacteria, Synergistetes, Spirochaetes and Caldiserica) except for the Chloroflexi. At the genus level, the influence of NPs on microbial abundance was significant. *Methanosaeta* were dominant in group A (75.25%), B (76.34%) and C (80.89%), but the abundance of *Methanosaeta* in reactors D and E was only 42.63% and 22.55%, respectively. In digestor A, B and C, the abundance of *Methanobacterium* was only 2.30–2.68%, while in digestor D, it was 26.13%, and in digestor E, it was the highest, accounting for 64.55%. *Proteiniclasticum*, *Clostridium_sensu_stricto_12* and *Christensenellaceae_R_7_group* were the top three abundant bacterial genera among five groups. As the predominant genus, the abundance of *Proteiniclasticum* in the digesters with NPs added were higher than that of the blank digesters.

The microbial Alpha-diversity indices (including Chao 1, ACE,

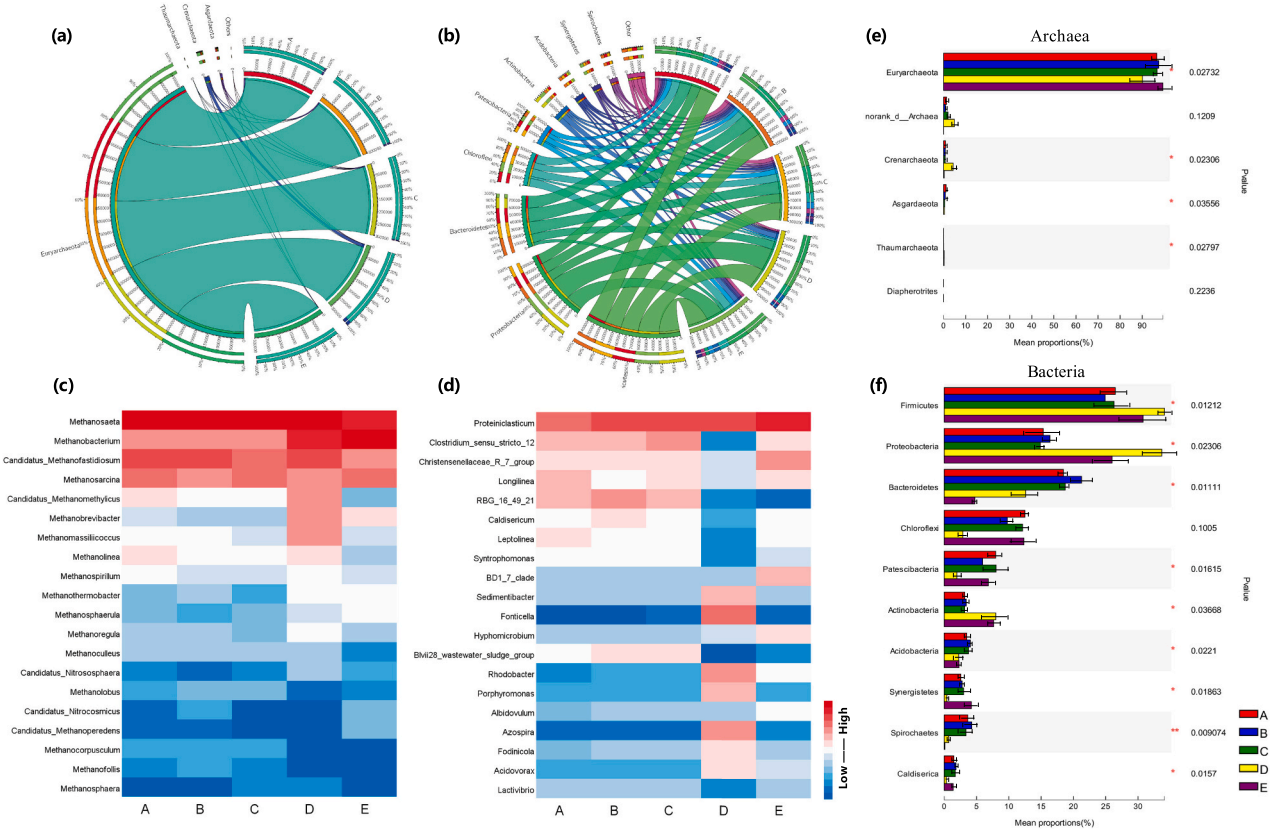


**Fig. 2.** The Circos graph showed the distribution of bacterial community (a) and archaea community (b) of five groups at phylum level. The heat-map revealed the evolution of top 20 bacterial genus (c) and archaea genus (d). Relative abundance of significantly different phylum among five groups. The Kruskal-Wallis H test was used to evaluate the importance of bacterial comparisons and archaea comparisons. *P < 0.05, **P < 0.01.

Shannon and Simpson) of the five groups (Table S3) showed that, the addition of carbon NPs and $Al_2O_3$ NPs decreased the bacterial diversity indices but increased the archaea diversity indices compared with the blank group. In the ZnO NPs group and CuO NPs group, the diversity index of bacteria and archaea was much lower than that of the blank group. These results partly explained that carbon NPs and $Al_2O_3$ NPs promoted the biogas production of AD, while ZnO NPs and CuO NPs inhibited the biogas production of AD. Partial least squares discriminant analysis (PLS-DA), a supervised analysis method, was used to reveal the differences among digesters with or without NPs added at phylum level. COMP1 and COMP2 explained 51.75% and 19.49% of the archaea composition variation, respectively (Fig. 3a). As for the bacterial composition, COMP1 and COMP2 explained 44.42% and 27.54% of the bacterial composition variation, respectively (Fig. 3b). It can be observed that the distances of microbial community among the group A, B and C were very close. Moreover, group D and group E had a long distance from the other three groups. The PLS-DA results explored that the microbial community among blank, carbon NPs and $Al_2O_3$ NPs digesters were similar. The community structure of bacteria and archaea in AD digester was significantly affected by CuO NPs and ZnO NPs.

In a previous study, it is found that carbon NPs can selectively enrich microorganisms participating in AD (Li et al., 2020; Lee et al., 2016). Carbon NPs significantly shorten the microbial contact distance and promote the direct interspecies electron transfer between the electricigens and methanogens. The electrogenic archaea *Methanobacterium* and *Methanospirillum* participate in the direct interspecies electron transfer mechanisms for the enhancement (Rotaru et al., 2014). The relative abundance of these genera was higher in the digester with carbon NPs added (2.52%) than in the control digester (2.30%). Due to the weak solubility of the $Al_2O_3$ NPs, the activity of methanogenic archaea was not be suppressed even when exposed to high level $Al_2O_3$ NPs, which indicated that the AD process could tolerate high concentrations of $Al_2O_3$ NPs (Yang et al., 2013). Carbon NPs and $Al_2O_3$ NPs have no obvious biological toxicity on microorganisms, so the microbial community in the group with the addition of carbon NPs and $Al_2O_3$ NPs were similar to those in the blank group. In the existence of CuO NPs and ZnO NPs, the reduction in microbial diversity was attributed to the bioavailable portion of the existed metal. CuO and ZnO are difficult to biodegrade, so they are easy to accumulate and reach the concentration with potential toxicity to microorganisms. The toxicity of CuO NPs and ZnO NPs to microbes was reflected in that they could induce microbial toxicity and damage microbial cell membranes. CuO NPs and ZnO NPs can not only be adsorbed on the microbial cell surface, but also produce reactive oxygen species when suspended in water. CuO NPs could produce superoxide anion and ZnO NPs could produce hydroxyl radicals (Applerot et al., 2009, 2012). Moreover, NPs could produce more reactive oxygen species due to their smaller particle size. Excessive production of active oxides induced by nano particles could cause oxidative stress leading to bacterial inactivation. Some of the CuO NPs and ZnO NPs with smaller particle size infiltrated into the microbial cells, which eventually led to the damage of microbial cells. Meanwhile, the increase of intracellular reactive oxygen species could damage the bacterial cell membrane and lead to bacterial cytoplasmic leakage (Xia et al., 2008). Moreover, reactive oxygen species are toxic to metabolites (such as protein and soluble polysaccharide) in AD process, which also explain that CuO NPs and ZnO NPs inhibited the methane generation and changed the microbial community structure. The difference between the microbial community structure of CuO NPs and ZnO NPs in AD reactors was mainly due to the different solubility of CuO NPs and ZnO NPs in sludge, which leads to different toxic effects on microorganisms (Wang et al., 2017).

### 3.4. Co-occurrence network between MGEs and bacteria

Co-occurrence network analysis was usually be used to reveal the potential hosts of the selected target genes in the complex environment. There were 98 nodes and 246 edges in the network. Fig. 4 showed that 87 bacterial genera (belonging to 6 phyla) were identified as the potential hosts for 11 targeted MGEs. All 98 nodes were clearly divided into four main modules. Module 1 showed that most bacterial genera were related to *tnpA*-02, *tnpA*-04, *tnpA*-07 and *IS*CR1. Module 2 only comprised *Tp*614 and *Roseomonas*. Module 3 consisted of potential hosts (*Brooklawnia*, *Dechlorobacter* and *Rhodoplanes*) related to *Tn*916/1545. Notably, module 4 showed that 5 selected MGEs (*IS*613, *tnpA*-01, *tnpA*-03, *tnpA*-05and *intI*1) had no correlation with potential hosts with relative abundances > 1% in this study. The numbers of potential host bacteria for *tnpA*-02, *IS*CR1 and *tnpA*-07 were relatively high at 69, 67 and 64, respectively. Additionally, different MGEs share common potential hosts, for example, the potential host bacteria *Acetonema* of *tnpA*-02, *tnpA*-04 and *tnpA*-07 were also possible hosts of *IS*CR1.

Most of these potential hosts, such as *Albidovulum*, *Defluviimonas* and *Acidovorax*, belong to the phylum Proteobacteria, which suggested that Proteobacteria played an important role in the variations and dissemination of MGEs during AD process with NPs added. *Acidovorax* is a member of antibiotic-resistant bacteria, it is known as the harboring transposases (Pala-Ozkok et al., 2019). In Fig. 2a, the abundances of Proteobacteria in the digesters with NPs added was higher than that of blank digester. The Proteobacteria abundance of the four experimental groups was 15.25% (carbon NPs), 15.20%, 16.08% and 16.00%, respectively, while that of the control group was 15.05%. In addition, Firmicutes has also been explored as a frequent host for selected MGEs. As the dominant bacterial genus, the abundance of *Proteiniclasticum* (Firmicutes) in ZnO NPs group (7.15%) and CuO NPs group (7.82%) was higher than that in the blank group (6.74%). *Proteiniclasticum*, a

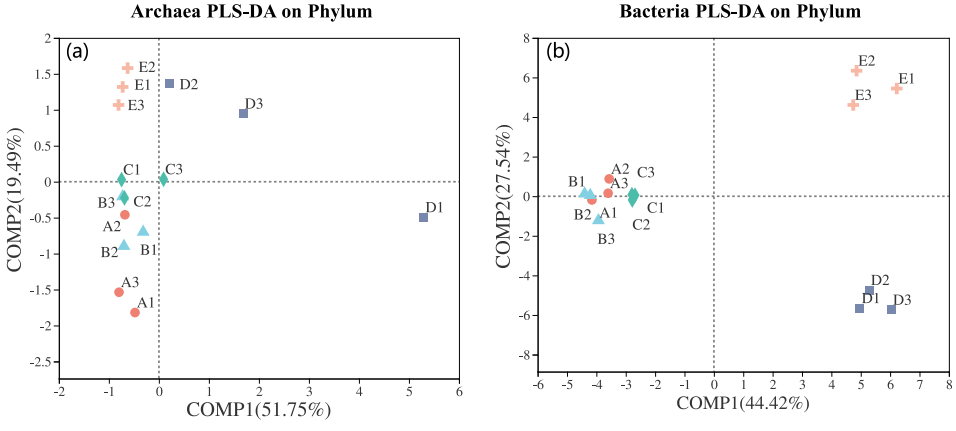


**Fig. 3.** Distribution of bacterial (a) and archaeal (b) community composition at genus level by PLS-DA.

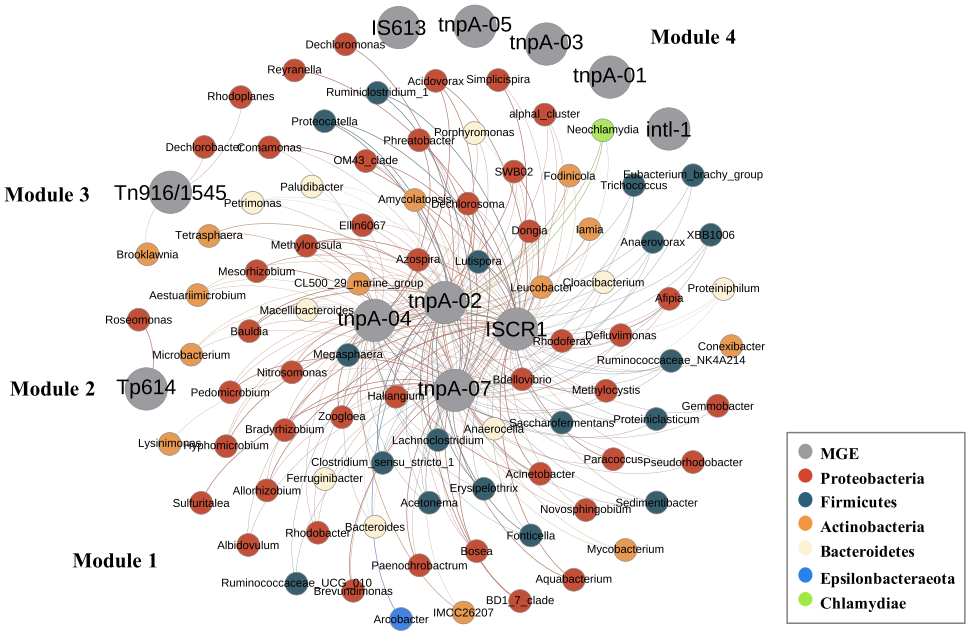


**Fig. 4.** Network analysis showed the co-occurrence patterns between the bacteria genus and MGEs. The thickness of arrows and lines was based on Pearson's correction coefficient.

bacterium able to digest proteins (Dong, 2010), is the potential host for *IS*CR1, *tnpA*-02 and *tnpA*-07. In ZnO NPs group, the abundance of *IS*CR1, *tnpA*-02 and *tnpA*-07 increased by 662.01%, 562.30% and 336.61%, respectively. In CuO NPs, the abundance of these three genes increased by 327.30%, 519.15% and 254.01%, respectively. A previous study showed that *Clostridium_sensu_stricto_1* and *Lachnoclostridium* belonged to Firmicutes were potential host bacteria of *Tn*916/1545 and *IS*CR1, which consist with another study (Wang et al., 2020). Changes of the potential host in the AD process generally synchronized with the evolution of MGEs. The addition of NPs in AD system led to the increase of host bacteria abundance, so that the enhance of MGEs abundance would be promoted. Therefore, network analysis further showed the bacteria community had a strong influence on the variation of MGEs.

It's worth noting that *Mycobacterium* and *Acinetobacter* are the two human pathogenic bacteria found in the study. *Mycobacterium*, a genus of Actinobacteria, is the cause of human tuberculosis (Dong, 2010). The overuse of antibiotics makes *Acinetobacter* acquire drug resistance and become "multi-drug resistance *Acinetobacter*". *Acinetobacter* has been considered as a "red alert" human pathogen because of its extensive antibiotic resistance spectrum (Chen et al., 2011). *Mycobacterium* is a potential host for *tnpA*-02 and *tnpA*-07. While, *Acinetobacter* is the potential host for *IS*CR1, *tnpA*-02 and *tnpA*-04. "Superbugs" may be generated when pathogenic bacteria acquire ARGs via HGT. Therefore, attention should be paid to NPs promote the HGT of multi resistance genes mediated by MGEs in AD process.

### 3.5. Effects of performance parameters on microorganisms and MGEs

#### 3.5.1. Response of microbial community to performance parameters

Redundancy analysis (RDA) was used to reveal the correlation between the AD performance parameters and the microbial communities in five groups. The abundance of the top 10 bacteria and archaea at genus level, as well as 9 performance parameters were selected for the RDA analysis. As shown in Fig. 5a, the two ordination axes of RDA jointly explained 97.9% of the bacterial community changes. The first and the second axes represented 95.0% and 2.9% variation of the microbial community, respectively. Distribution of samples appeared a significant evolution. Blank group, carbon NPs and $Al_2O_3$ NPs group

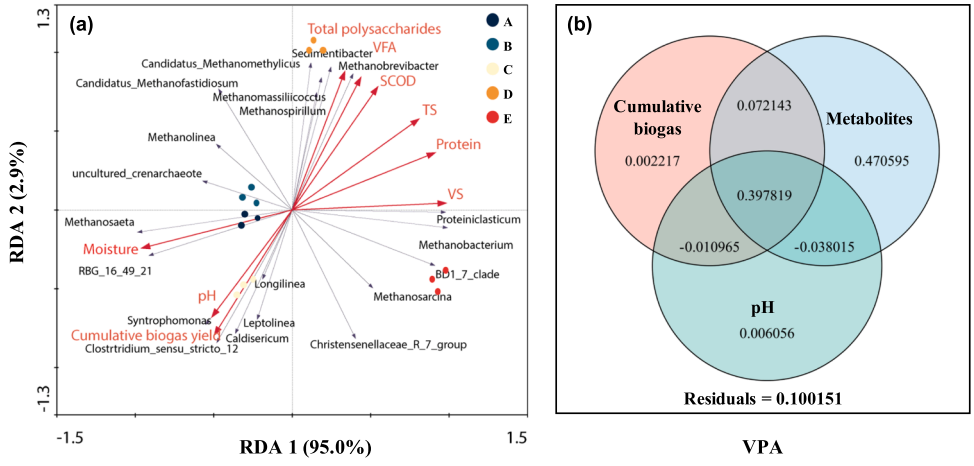


**Fig. 5.** Redundancy analysis (RDA) based on Bray-Curtis distance illustrated the correlation of performance parameters with bacterial community (genus level) in the five groups (a). Variation partitioning analysis (VPA) analysis of bacterial community variations explained by performance parameters (b).

were clustered closely, while the samples of ZnO NPs group and CuO NPs group had a great distance. The results of RDA and PLS-DA were consistent.

The performance parameters were mainly distributed in two quadrants and there was a positive correlation between performance parameters in the same quadrant. Total polysaccharides, VFA, SCOD, proteins, TS and VS were clustered closely. Moisture, pH, and cumulative biogas yield were very close in the other quadrant. It is worth mentioning that, the metabolites in the reactor had been consumed by microorganisms at the end of the AD, while the accumulative gas production reached the maximum yield. The more thoroughly the metabolites were consumed, the higher the cumulative gas production. Therefore, the cumulative biogas yield is inversely proportional to the metabolites in RDA, which was coincided with above discussion. The distribution of microbial communities can be also revealed in RDA results. Most archaea were directly proportional to metabolites, they played an important role in converting metabolites into methane. But these archaea were inversely proportional to pH and moisture. *Methanosaeta* and *Methanobacterium* are the important methanogenic bacterium, which are positively relationship with accumulative biogas yield. These two methanogens may participate in the methanogenesis process in AD process. The dominant bacterial genus *Proteiniclasticum* also had a positive response to metabolites, TS and VS. Most other bacterial genus, such as *Clostridium_sensu_stricto_12*, *Christensenellaceae_R_7_group*, and *Longilinea* were located near the arrow of biogas production indicating that they had a significant effect on biogas accumulation.

To explore the statistical significance of the performance parameters affecting bacterial community, the Mantel test based on Bray-Curtis distance revealed that there was a remarkable correlation between the performance parameters and the bacterial community ($R = 0.956$, $P = 0.001$). Variation partitioning analysis (VPA) can further explain the putative interactions among species, functions and samples (Xiang et al., 2018). The AD performance parameters were divided into three groups: metabolites, pH, and accumulative biogas yield. The metabolites included SCOD, total polysaccharides, protein and VFA. The changes of bacterial community in this study were more attributed to metabolites (47.06%) shift than that of biogas (0.22%) and pH (0.61%) revealed by VPA (Fig. 5b), while the combined effects of the AD performance parameters accounted for 39.78%. The results of VPA suggested that metabolites may be an important driver of bacterial community in the AD process. At the same time, it also shows that the performance parameters affecting the bacterial community were interdependent in the AD system.

### 3.5.2. Response of MGEs to AD performance parameters

To understand the interconnections between AD performance parameters and MGEs, Spearman's rank correlation analysis was conducted in the five AD groups (Fig. 6). In this case, all the environmental variables didn't have significant relationships with *IS*613, *Tp*614, *Tn*916/1545 and *int*I1. For the remaining MGEs, performance parameters are divided into two categories: one is negatively correlated with these MGEs (including pH, gas production and moisture), the other is positively correlated with these genes (including TS, VS, SCOD, total polysaccharides, protein and VFA). pH was significantly negatively correlated with nearly half of the MGEs, and the cumulative gas production rate was only significantly negatively correlated with *tnpA*-03 ($R = -0.885$, $P = 0.046$). TS was significantly positively correlated with *tnpA*-04 ($R = 0.882$, $P = 0.048$) and *IS*CR1 ($R = 0.905$, $P = 0.035$), respectively. Moreover, the four metabolites were significantly correlated with *tnpA*-01, *tnpA*-02, *tnpA*-03, *tnpA*-04, *tnpA*-05, *tnpA*-07 and *IS*CR1. The bacterial communities varied in response to AD performance parameters. The addition of different NPs resulted in different performance parameters during AD process. The number of specific bacteria carrying MGEs changed in AD system with NPs added, which indirectly alter the abundance of MGEs (Zhang et al., 2019a). The results of VPA showed that the metabolites were the dominant factors affecting bacterial community, suggesting that the metabolites are the key determinant of MGEs in AD process.

## 4. Conclusions

The present study evaluated different effects of four NPs (carbon NPs, $Al_2O_3$ NPs, ZnO NPs, and CuO NPs) on the removal/enhance of MGEs in AD system. The microbial community variety and the potential host of the MGEs were also explored in this study. Carbon NPs and $Al_2O_3$ NPs could promote the biogas production of AD, while ZnO NPs and CuO NPs could inhibit biogas production. Nevertheless, the four NPs reduced the bacterial diversity. Carbon NPs and $Al_2O_3$ NPs increased the archaea diversity, while ZnO NPs and CuO NPs decreased the archaea diversity. Compared with carbon NPs and $Al_2O_3$ NPs, ZnO NPs and CuO NPs have

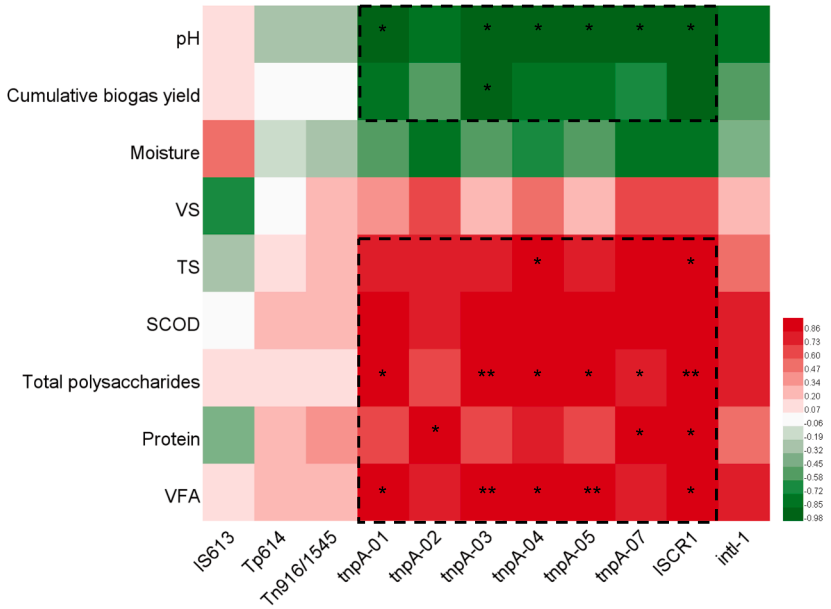


**Fig. 6.** Heatmap based on the relationship between MGEs and performance parameters. Color intensity shows the correlation between each factor, as shown by the color key at the bottom right.

more significant influence on the variety of microbial community structure. The qPCR results showed that the abundance of MGEs were significantly enriched in the digesters with conductive NPs added. Co-occurrence network analysis showed that 87 bacterial genera (belong to 6 phyla) exhibited relative abundance greater than 1% and they were considered as potential host bacteria of MGEs. Proteobacteria and Firmicutes were the main potential hosts of MGEs. Metabolites (total polysaccharides, VFA, SCOD and proteins) were the most important parameters influencing bacterial community changes, and the amount of explanation for bacterial community variation was 47.06%. The bacterial communities that may carry MGEs respond differently to environmental factors. Therefore, metabolites were also significantly positively correlated with some MGEs in this study. Overall, this study forewarns that the release of NPs could be contribute to the propagation of ARGs via MGEs in sludge AD system.

## CRediT authorship contribution statement

**Yanru Zhang**: Writing - original draft, Writing - review & editing, Data curation, Formal analysis. **Rui Xu**: Writing - review & editing, software, Formal analysis. **Yinping Xiang**: Writing - review & editing, software. **Yue Lu**: Writing - review & editing, software. **Meiying Jia**: Writing - review & editing. **Jing Huang**: Writing - review & editing. **Zhengyong Xu**: Writing - review & editing. **Jiao Cao**: Writing - review & editing. **Weiping Xiong**: conceptualization, supervision, project administration. **Zhaohui Yang**: Writing - review & editing.

## Declaration of Competing Interest

The authors declare that they have no known competing financial interests or personal relationships that could have appeared to influence the work reported in this paper.

## Acknowledgements

The study was financially supported by the China and National Natural Science Foundation of China (51878258, 51521006 and 51709100). We would like to thank Yawen Chen for her contribution to the experimental operation and data analysis.

## Appendix A. Supporting information

Supplementary data associated with this article can be found in the online version at doi:10.1016/j.jhazmat.2020.124206.

## References

Applerot, G., Lipovsky, A., Dror, R., Perkas, N., Nitzan, Y., Lubart, R., Gedanken, A., 2009. Enhanced antibacterial activity of nanocrystalline ZnO due to increased ROS-mediated cell injury. Adv. Funct. Mater. 19, 842–852.

Applerot, G., Lellouche, J., Lipovsky, A., Nitzan, Y., Lubart, R., Gedanken, A., Banin, E., 2012. Understanding the antibacterial mechanism of CuO nanoparticles: revealing the route of induced oxidative stress. Small 8, 3326–3337.

Chen, C.-C., Lin, Y.-C., Sheng, W.-H., Chen, Y.-C., Chang, S.-C., Hsia, K.-C., Liao, M.-H., Li, S.-Y., 2011. Genome sequence of a dominant, multidrug-resistant Acinetobacter baumannii strain, TCDC-AB0715. J. Bacteriol. 193, 2361–2362.

Dhariwal, A., Chong, J., Habib, S., King, I.L., Agellon, L.B., Xia, J., 2017. Microbiome analyst: a web-based tool for comprehensive statistical, visual and meta-analysis of microbiome data. Nucleic Acids Res. 45, W180–W188.

Di Cesare, A., Eckert, E.M., D'Urso, S., Bertoni, R., Gillan, D.C., Wattiez, R., Corno, G., 2016. Co-occurrence of integrase 1, antibiotic and heavy metal resistance genes in municipal wastewater treatment plants. Water Res. 94, 208–214.

Dong, X., 2010. Proteiniclasticum ruminis gen. nov., sp. nov., a strictly anaerobic proteolytic bacterium isolated from yak rumen. Int. J. Syst. Evolut. Microbiol. 60, 2221–2225.

Gillings, M., Boucher, Y., Labbate, M., Holmes, A., Krishnan, S., Holley, M., Stokes, H.W., 2008. The evolution of class 1 integrons and the rise of antibiotic resistance. J. Bacteriol. 190, 5095–5100.

Gonzalez-Estrella, J., Sierra-Alvarez, R., Field, J.A., 2013. Toxicity assessment of inorganic nanoparticles to acetoclastic and hydrogenotrophic methanogenic activity in anaerobic granular sludge. J. Hazard. Mater. 260, 278–285.

Hall, R.M., Stokes, H.W., 1993. Integrons: novel DNA elements which capture genes by site-specific recombination. Genetica 90, 115–132.

Harshey, R.M., 2003. Bacterial motility on a surface: many ways to a common goal. Annu. Rev. Microbiol. 57, 249–273.

Huang, H., Chen, Y., Yang, S., Zheng, X., 2019. CuO and ZnO nanoparticles drive the propagation of antibiotic resistance genes during sludge anaerobic digestion: possible role of stimulated signal transduction. Environ. Sci. Nano 6, 528–539.

Kaiser, D., 2000. Bacterial motility: How do pili pull? Curr. Biol. 10, R777–R780.

Kapoor, V., Phan, D., Pasha, A.B.M.T., 2018. Effects of metal oxide nanoparticles on nitrification in wastewater treatment systems: a systematic review. J. Environ. Sci. Health Part A 53, 659–668.

Lee, J.Y., Lee, S.H., Park, H.D., 2016. Enrichment of specific electro-active microorganisms and enhancement of methane production by adding granular activated carbon in anaerobic reactors. Bioresour. Technol. 205, 205–212.

Li, L., Zhang, X., Zhu, P., Yong, X., Wang, Y., An, W., Jia, H., Zhou, J., 2020. Enhancing biomethane production and pyrene biodegradation by addition of bio-nano FeS or magnetic carbon during sludge anaerobic digestion. Environ. Technol. 1–12.

Liu, X., Xu, Q., Wang, D., Wu, Y., Yang, Q., Liu, Y., Wang, Q., Li, X., Li, H., Zeng, G., Yang, G., 2019a. Unveiling the mechanisms of how cationic polyacrylamide affects short-chain fatty acids accumulation during long-term anaerobic fermentation of waste activated sludge. Water Res. 155, 142–151.

Liu, X., Tang, J., Song, B., Zhen, M., Wang, L., Giesy, J.P., 2019b. Exposure to $Al_2O_3$ nanoparticles facilitates conjugative transfer of antibiotic resistance genes from Escherichia coli to Streptomyces. Nanotoxicology 13, 1422–1436.

Liu, X., Huang, X., Wu, Y., Xu, Q., Du, M., Wang, D., Yang, Q., Liu, Y., Ni, B.-J., Yang, G., Yang, F., Wang, Q., 2020. Activation of nitrite by freezing process for anaerobic digestion enhancement of waste activated sludge: performance and mechanisms. Chem. Eng. J. 387, 124147.

Mu, H., Chen, Y., 2011. Long-term effect of ZnO nanoparticles on waste activated sludge anaerobic digestion. Water Res. 45, 5612–5620.

Mu, H., Chen, Y., Xiao, N., 2011. Effects of metal oxide nanoparticles (TiO2, $Al_2O_3$, SiO2 and ZnO) on waste activated sludge anaerobic digestion. Bioresour. Technol. 102, 10305–10311.

Nolivos, S., Cayron, J., Dedieu, A., Page, A., Delolme, F., Lesterlin, C., 2019. Role of AcrAB-TolC multidrug efflux pump in drug-resistance acquisition by plasmid transfer. Science 364, 778–782.

Okitsu, N., Kaieda, S., Yano, H., Nakano, R., Hosaka, Y., Okamoto, R., Kobayashi, T., Inoue, M., 2005. Characterization of ermB gene transposition by Tn1545 and Tn917 in macrolide-resistant Streptococcus pneumoniae isolates. J. Clin. Microbiol 43, 168–173.

Pala-Ozkok, Ilke, Ubay-Cokgor, Emine, Jonas, Daniel, Orhon, Derin, 2019. Kinetic and microbial response of activated sludge community to acute and chronic exposure to tetracycline. J. Hazard. Mater. 367, 418–426.

Partridge, S.R., Kwong, S.M., Neville, F., Jensen, S.O., 2018a. Mobile genetic elements associated with antimicrobial resistance. Clin. Microbiol. Rev. 31.

Partridge, S.R., Kwong, S.M., Firth, N., Jensen, S.O., 2018b. Mobile genetic elements associated with antimicrobial resistance. Clin. Microbiol. Rev. 31 e00088-00017.

Qiu, Z., Yu, Y., Chen, Z., Jin, M., Yang, D., Zhao, Z., Wang, J., Shen, Z., Wang, X., Qian, D., 2012. Nanoalumina promotes the horizontal transfer of multiresistance genes mediated by plasmids across genera. Proc. Natl. Acad. Sci. USA 109, 4944–4949.

Rizzo, L., Manaia, C., Merlin, C., Schwartz, T., Dagot, C., Ploy, M.C., Michael, I., Fatta-Kassinos, D., 2013. Urban wastewater treatment plants as hotspots for antibiotic resistant bacteria and genes spread into the environment: a review. Sci. Total Environ. 447, 345–360.

Rotaru, A., Shrestha, P.M., Liu, F., Markovaite, B., Chen, S., Nevin, K.P., Lovley, D.R., 2014. Direct interspecies electron transfer between Geobacter metallireducens and Methanosarcina barkeri. Appl. Environ. Microbiol. 80, 4599–4605.

Sun, L., Ding, Y., Yang, B., He, N., Chen, T., 2020. Effect of biological powdered activated carbon on horizontal transfer of antibiotic resistance genes in secondary effluent. Environ. Eng. Sci. 37, 365–372.

Sun, T.Y., Bornhoft, N.A., Hungerbuhler, K., Nowack, B., 2016. Dynamic probabilistic modeling of environmental emissions of engineered nanomaterials. Environ. Sci. Technol. 50, 4701–4711.

Toleman, M.A., Bennett, P.M., Walsh, T.R., 2006. ISCR elements: novel gene-capturing systems of the 21st century? Microbiol. Mol. Biol. Rev. 70, 296–316.

Vodovnik, M., Kostanjsek, R., Zorec, M., Marinsek Logar, R., 2012. Exposure to $Al_2O_3$ nanoparticles changes the fatty acid profile of the anaerobe Ruminococcus flavefaciens. Folia Microbiol. 57, 363–365.

W.H. Organization, WHO, 2015. Global action plan on antimicrobial resistance.

Wallace, J.S., Garner, E., Pruden, A., Aga, D.S., 2018. Occurrence and transformation of veterinary antibiotics and antibiotic resistance genes in dairy manure treated by advanced anaerobic digestion and conventional treatment methods. Environ. Pollut. 236, 764–772.

Wang, P., Chen, X., Liang, X., Cheng, M., Ren, L., 2019. Effects of nanoscale zero-valent iron on the performance and the fate of antibiotic resistance genes during thermophilic and mesophilic anaerobic digestion of food waste. Bioresour. Technol. 293, 122092.

Wang, Q., Gu, J., Wang, X., Ma, J., Hu, T., Peng, H., Bao, J., Zhang, R., 2020. Effects of nano-zerovalent iron on antibiotic resistance genes and mobile genetic elements during swine manure composting. Environ. Pollut. 258, 113654.

Wang, S., Li, Z., Gao, M., She, Z., Guo, L., Zheng, D., Zhao, Y., Ma, B., Gao, F., Wang, X., 2017. Long-term effects of nickel oxide nanoparticles on performance, microbial enzymatic activity, and microbial community of a sequencing batch reactor. Chemosphere 169, 387–395.

Wang, X.L., Yang, F.X., Zhao, J., Xu, Y., Mao, D.Q., Zhu, X., Luo, Y., Alvarez, P.J.J., 2018. Bacterial exposure to ZnO nanoparticles facilitates horizontal transfer of antibiotic resistance genes. Nanoimpact 10, 61–67.

Wösten, M.M.S.M., Kox, L.F.F., Chamnongpol, S., Soncini, F.C., Groisman, E.A., 2000. A signal transduction system that responds to extracellular iron. Cell 103, 113–125.

Xia, T., Kovochich, M., Liong, M., Mädler, L., Gilbert, B., Shi, H., Yeh, J.I., Zink, J.I., Nel, A.E., 2008. Comparison of the mechanism of toxicity of zinc oxide and cerium oxide nanoparticles based on dissolution and oxidative stress properties. ACS Nano 2, 2121–2134.

Xiang, Q., Chen, Q.L., Zhu, D., An, X.L., Yang, X.R., Su, J.Q., Qiao, M., Zhu, Y.G., 2018. Spatial and temporal distribution of antibiotic resistomes in a peri-urban area is associated significantly with anthropogenic activities. Environ. Pollut. 235, 525–533.

Xiang, Y., Yang, Z., Zhang, Y., Xu, R., Zheng, Y., Hu, J., Li, X., Jia, M., Xiong, W., Cao, J., 2019. Influence of nanoscale zero-valent iron and magnetite nanoparticles on anaerobic digestion performance and macrolide, aminoglycoside, beta-lactam resistance genes reduction. Bioresour. Technol. 294, 122139.

Xu, R., Yang, Z., Zheng, Y., Zhang, H., Liu, J., Xiong, W., Zhang, Y., Ahmad, K., 2017. Depth-resolved microbial community analyses in the anaerobic co-digester of dewatered sewage sludge with food waste. Bioresour. Technol. 244, 824–835.

Xu, R., Yang, Z., Wang, Q., Bai, Y., Liu, J., Zheng, Y., Zhang, Y., Xiong, W., Ahmad, K., Fan, C., 2018a. Rapid startup of thermophilic anaerobic digester to remove tetracycline and sulfonamides resistance genes from sewage sludge. Sci. Total Environ. 612, 788–798.

Xu, R., Yang, Z.-H., Wang, Q.-P., Bai, Y., Liu, J.-B., Zheng, Y., Zhang, Y.-R., Xiong, W.-P., Ahmad, K., Fan, C.-Z., 2018b. Rapid startup of thermophilic anaerobic digester to remove tetracycline and sulfonamides resistance genes from sewage sludge. Sci. Total Environ. 612, 788–798.

Xu, R., Xu, S., Florentino, A.P., Zhang, L., Yang, Z., Liu, Y., 2019. Enhancing blackwater methane production by enriching hydrogenotrophic methanogens through hydrogen supplementation. Bioresour. Technol. 278, 481–485.

Xu, R., Li, B., Xiao, E., Young, L.Y., Sun, X., Kong, T., Dong, Y., Wang, Q., Yang, Z., Chen, L., Sun, W., 2020a. Uncovering microbial responses to sharp geochemical gradients in a terrace contaminated by acid mine drainage. Environ. Pollut. 261, 114226.

Xu, R., Zhang, Y., Xiong, W., Sun, W., Fan, Q., Zhaohui, Y., 2020c. Metagenomic approach reveals the fate of antibiotic resistance genes in a temperature-raising anaerobic digester treating municipal sewage sludge. J. Clean. Prod. 277, 123504.

Xu, Y., Wang, M., Yu, Q., Zhang, Y., 2020b. Enhancing methanogenesis from anaerobic digestion of propionate with addition of Fe oxides supported on conductive carbon cloth. Bioresour. Technol. 302, 122796.

Yan, W., Xiao, Y., Yan, W., Ding, R., Wang, S., Zhao, F., 2019. The effect of bioelectrochemical systems on antibiotics removal and antibiotic resistance genes: a review. Chem. Eng. J. 358, 1421–1437.

Yan, W., Bai, R., Wang, S., Tian, X., Li, Y., Wang, S., Yang, F., Xiao, Y., Lu, X., Zhao, F., 2020. Antibiotic resistance genes are increased by combined exposure to sulfamethoxazole and naproxen but relieved by low-salinity. Environ. Int. 139, 105742.

Yang, Y., Zhang, C., Hu, Z., 2013. Impact of metallic and metal oxide nanoparticles on wastewater treatment and anaerobic digestion. Environ. Sci. Process Impacts 15, 39–48.

Yang, Y., Zhang, Y., Li, Z., Zhao, Z., Quan, X., Zhao, Z., 2017. Adding granular activated carbon into anaerobic sludge digestion to promote methane production and sludge decomposition. J. Clean. Prod. 149, 1101–1108.

Yuan, Q., He, Y., Mao, B., Zuo, P., Wu, W., Huang, Y., Javed, H., Hu, N., 2020. Nano-metal oxides naturally attenuate antibiotic resistance in wastewater: killing antibiotic resistant bacteria by dissolution and decreasing antibiotic tolerance by attachment. NanoImpact 18, 100225.

Yuan, X., Zhang, X., Sun, L., Wei, Y., Wei, X., 2019. Cellular toxicity and immunological effects of carbon-based nanomaterials. Part. Fibre Toxicol. 16, 18.

Zhang, L., He, X., Zhang, Z., Cang, D., Nwe, K.A., Zheng, L., Li, Z., Cheng, S., 2017. Evaluating the influences of ZnO engineering nanomaterials on VFA accumulation in sludge anaerobic digestion. Biochem. Eng. J. 125, 206–211.

Zhang, R., Gu, J., Wang, X., Li, Y., Liu, J., Lu, C., Qiu, L., 2019a. Response of antibiotic resistance genes abundance by graphene oxide during the anaerobic digestion of swine manure with copper pollution. Sci. Total Environ. 654, 292–299.

Zhang, Y., Yang, Z., Xu, R., Xiang, Y., Jia, M., Hu, J., Zheng, Y., Xiong, W., Cao, J., 2019b. Enhanced mesophilic anaerobic digestion of waste sludge with the iron nanoparticles addition and kinetic analysis. Sci. Total Environ. 683, 124–133.

Zhang, Y., Yang, Z., Xiang, Y., Xu, R., Zheng, Y., Lu, Y., Jia, M., Sun, S., Cao, J., Xiong, W., 2020. Evolutions of antibiotic resistance genes (ARGs), class 1 integron-integrase (*intI*1) and potential hosts of ARGs during sludge anaerobic digestion with the iron nanoparticles addition. Sci. Total Environ. 724, 138248.

Zhu, Y.-G., Zhao, Y., Li, B., Huang, C.-L., Zhang, S.-Y., Yu, S., Chen, Y.-S., Zhang, T., Gillings, M.R., Su, J.-Q., 2017. Continental-scale pollution of estuaries with antibiotic resistance genes. Nat. Microbiol. 2, 16270.